REPORT DOCUMENTATION PAGE

Form Approved
OMB No. 0704-0188

1. REPORT DATE *(DD-MM-YYYY)*	**2. REPORT TYPE**	**3. DATES COVERED** *(From - To)*
19-03-2008	Technical Paper	

4. TITLE AND SUBTITLE

Atomization Rate of Gas-Centered Swirl-Coaxial Injectors (Preprint)

5a. CONTRACT NUMBER

5b. GRANT NUMBER

5c. PROGRAM ELEMENT NUMBER

6. AUTHOR(S)
Malissa D.A. Lightfoot, Stephen A. Danczyk, & Douglas G. Talley (AFRL/RZSA)

5d. PROJECT NUMBER

5e. TASK NUMBER
50260538

5f. WORK UNIT NUMBER

7. PERFORMING ORGANIZATION NAME(S) AND ADDRESS(ES)

Air Force Research Laboratory (AFMC)
AFRL/RZSA
10 E. Saturn Blvd.
Edwards AFB CA 93524-7680

8. PERFORMING ORGANIZATION REPORT NUMBER

AFRL-RZ-ED-TP-2008-074

9. SPONSORING / MONITORING AGENCY NAME(S) AND ADDRESS(ES)

Air Force Research Laboratory (AFMC)
AFRL/RZS
5 Pollux Drive
Edwards AFB CA 93524-7048

10. SPONSOR/MONITOR'S ACRONYM(S)

11. SPONSOR/MONITOR'S NUMBER(S)
AFRL-RZ-ED-TP-2008-074

12. DISTRIBUTION / AVAILABILITY STATEMENT

Approved for public release; distribution unlimited (PA #08125A).

13. SUPPLEMENTARY NOTES
Submitted for presentation at the 21st ILASS-Americas Meeting, to be held in Orlando, FL, 18-21 May 2008.

14. ABSTRACT

Gas-centered swirl-coaxial injectors are garnering much interest in the area of liquid hydrocarbon rocket development. However, robust design criteria and scaling of these injectors remains unclear. Here an examination of primary atomization has been undertaken through the study of a gas-centered swirl-coaxial injector. Film length is measured experimentally over a range of operating conditions and injector geometries. Experiments are performed at atmospheric pressure using water and nitrogen as working fluids. The atomization rate, reflected in the length of the intact liquid film, is related to the momentum flux ratio. Using the characteristic dimensions for determining the bulk velocities of the fluids, the film lengths of various injector geometries may be collapsed onto a single curve of nondimensionalized length versus momentum flux ratio. The injectors tested have a geometry which produces separated gas flow just prior to contact with the liquid. The effect of this recirculation zone on initial film height is discussed.

15. SUBJECT TERMS

16. SECURITY CLASSIFICATION OF:			**17. LIMITATION OF ABSTRACT**	**18. NUMBER OF PAGES**	**19a. NAME OF RESPONSIBLE PERSON**
					Dr. Stephen Danczyk
a. REPORT	**b. ABSTRACT**	**c. THIS PAGE**	SAR	9	**19b. TELEPHONE NUMBER** *(include area code)*
Unclassified	**Unclassified**	**Unclassified**			N/A

Atomization Rate of Gas-Centered Swirl-Coaxial Injectors (Preprint)

M.D.A. Lightfoot*, S.A. Danczyk and D.G. Talley
Air Force Research Laboratory
Edwards Air Force Base
Edwards AFB, CA 93524-7660 USA

Abstract

Gas-centered swirl-coaxial injectors are garnering much interest in the area of liquid hydrocarbon rocket development. However, robust design criteria and scaling of these injectors remains unclear. Here an examination of primary atomization has been undertaken through the study of a gas-centered swirl-coaxial injector. Film length is measured experimentally over a range of operating conditions and injector geometries. Experiments are performed at atmospheric pressure using water and nitrogen as working fluids. The atomization rate, reflected in the length of the intact liquid film, is related to the momentum flux ratio. Using the characteristic dimensions for determining the bulk velocities of the fluids, the film lengths of various injector geometries may be collapsed onto a single curve of nondimensionalized length versus momentum flux ratio. The injectors tested have a geometry which produces separated gas flow just prior to contact with the liquid. The effect of this recirculation zone on initial film height is discussed.

*Corresponding author, malissa.lightfoot@edwards.af.mil

Introduction

In recent years gas-centered swirl-coaxial (GCSC) injectors have attracted much attention for use in rocket engines. When used in liquid hydrocarbon-gaseous oxygen combustion chambers, GCSC injectors have some distinct advantages over other commonly used injector types. Their use in American systems has been limited, however. Curently, the best design practices for these injectors is unknown and relevant scaling in both size and from cold-flow to combusting-flow remains unclear [1-3].

Gas-centered swirl-coaxial injectors have characteristics of both pressure-swirl (e.g. a swirl chamber) and swirl-coaxial (e.g. strong shearing forces) injectors but are unique from both. A basic schematic of a GCSC injector is given in Fig. 1. Liquid enters small inlet ports drilled tangential to the cylindrical outlet section. Unswirled gas enters through the center of the injector. In some GCSC atomizers, such as the ones examined here, a short section exists where the liquid is sheltered from the gas. This sheltered region allows the liquid flow to develop before coming in contact with the gas. However, the wall separating the gas and liquid introduces some additional complexities, particularly due to its blunt end: the sudden expansion following the wall will produce a separated flow region in the gas.

GCSC injectors are effective atomizers due to the energetic gas flow along their centerlines. Because their atomization process is gas-dominated, it has been hypothesized that a stripping mechanism dominated by gas-phase turbulence is the main process by which droplets are produced [4]. From this hypothesis and studies of other injectors with strong gas flows, it is expected that the film length, a measure of the volumetric rate of atomization (hereafter atomization rate), will scale with the ratio of the momentum fluxes of the two fluids [4-7]. However, the existence of the sheltering lip and the subsequent separated flow can reasonably be expected to affect the atomization. The exact consequences of the sudden expansion, in terms of resultant film length, are unclear: the lower pressure created by the recirculating flow will cause an increase in film thickness (thus in film surface area), but the film length in this region seems to be less dependent on the bulk gas flow.

A parametric study of injector geometry was undertaken to ascertain if film length does indeed scale with momentum flux ratio and the correct dimensions to use in this scaling. The study also aims to answer some of the questions regarding the effect of the sheltering lip on film length.

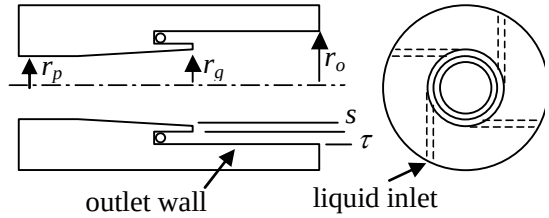

Figure 1: In this schematic of a gas-centered swirl-coaxial injector r_p represents the initial gas post radius, r_g the gas radius at the end of the sheltering lip, r_o the outlet radius, s the step height and τ the gap height. Table 1 lists the values of these dimensions used in the experiments.

Insert	r_o	s	τ	r_g
	mm	mm	mm	mm
1	9.525	1.19	1.98	6.35
2	9.525	0.41	1.65	7.47
3	9.525	2.74	1.32	5.46
4	9.525	1.52	1.65	6.35

Table 1: Dimensions of the injector inserts used in these experiments are given.

Experimental Set-up

A modular GCSC injector was designed for these experiments and is illustrated in Fig. 1 with variable dimensions given in Table 1. The gas plenum and gas post of this injector are stainless steel; the gas post (r_p) is 152 mm (6") in length and 12.7 mm (0.5") in diameter. The outlet is constructed from polished polycarbonate; this section is what is illustrated in Fig. 1. The outlet piece may be replaced to alter the outlet diameter, the liquid inlet area or arrangement of inlet holes; in the current investigation only one outlet piece was used. The outlet (r_o) was 19.1 mm (0.75") in diameter with 4 inlet holes 0.775 mm (0.0305") in diameter. A removable insert allows the initial liquid thickness (also called the liquid gap; τ in Fig. 1) and the sheltering lip height (also referred to as step height; s in Fig. 1) to be varied; obviously, changes in these two dimensions affect the diameter of the gas post prior to liquid contact (r_g). Four inserts were examined in these experiments; their relevant dimensions can be found in Table 1. For all inserts

the length of the sheltered area was 3.18 mm (0.125").

All of these experiments were conducted at atmospheric pressure. The working fluids were water and nitrogen. Flow rates were regulated with an upstream cavitating venturi and sonic nozzle, for the liquid and gas respectively. A specified flow rate was achieved by setting the supply pressure of the fluids. Both the venturi and sonic nozzle were calibrated using a capture-and-weigh technique; with this calibration and the pressure transducers used to measure the supply pressure, flow rates are accurate to $+/1.36 \times 10^{-4}$ kg/s. A valve downstream of the venturi (but upstream of the injector) insured that there was sufficient back pressure to minimize acoustic noise.

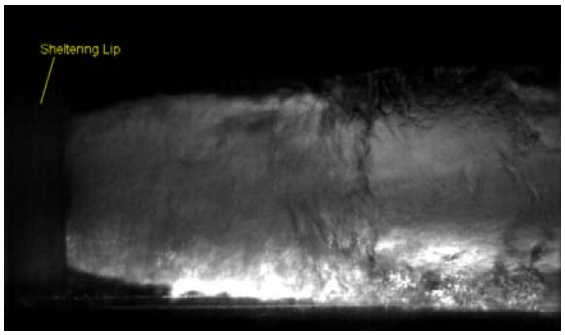

Figure 2: This is a typical image from the high speed camera. Gas enters from the left. The bottom interface is the one measured; the top interface is heavily shadowed.

An Argon-ion laser and cylindrical lens were used to produce a laser sheet. This sheet was introduced along the central axis of the injector. A Phantom v7.3 camera was positioned 90° from this laser sheet. Images of the injector outlet were recorded at 1000 frames per second. The length of the liquid film and a film height near the sheltered lip were measured from these images across the center-plain of the injector. Attenuation through the rough interface and droplets in the core of the injector resulted in a heavily shadowed view of the interface opposite the laser; the data reported here were measured from the near-laser interface only. A typical image is given in Fig. 2; the lower interface is the near-laser interface in this figure. Due to variations in the lighting and very thin liquid films, measurements of the film length and height were made by hand. The only image processing performed was altering the contrast and brightness to enhance the visibility of the interface. Measurements were made of every 10 frames, essentially providing data every 0.01 seconds. One second's worth of data, i.e. 100 images, were averaged to get the values reported here. The reported film height near the step, *h*, was measured approximately 0.940 mm (0.037") downstream of the sheltered area.

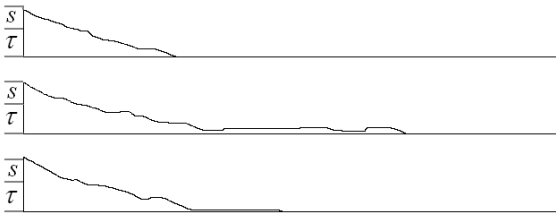

Figure 3: The film thickness may be very small for some distance. An error in the location of the outside wall of the injector may shorten the measured length a little in some tests and a lot in others. The images here are for insert 1 at $\Phi_{\tau,rg}$=823.

There are two main complications affecting these measurements. The first difficulty is that the boundary between gas and liquid is rarely crisp: instead of one pixel being white and the next black, there is a band of several progressively lighter pixels within which the gas-liquid interface is located. This is the main source of error in the height measurements (+/-0.31 mm) and exists not only for the film but also, to a lesser extent, when determining the location of the outlet wall in the images. Changes in the refractive index when a film is present prevent using the brighter, no liquid images to determine the exact location of the outlet wall in the images where a liquid film is present. The second complication, the main source of error in the length measurements, occurs as a result of the film thinning. The interface between the liquid and gas is very chaotic and does not smoothly decrease in thickness. Due to differences in initial film height and different atomization rates, the liquid also thins at a different rate in each test. At some momentum flux ratios the film is very thin for a long distance while at others, the film abruptly decreases in thickness. While variable with operating condition and geometry, the thinning rate is repeatable at the same geometry and condition. Figure 3 shows a few representative traces of a film profile at one operating condition. This figure illustrates how the film length can vary if the location of the outlet wall is incorrectly selected in the images. From this figure it is obvious that moving the selected wall location up or down one pixel changes the film

	Mass Flow Rates (kg/s)		Momentum Flux Ratio		
Insert	m_g	m_l	$\Phi_{\tau,rg}$	$\Phi_{\tau,rg+s}$	$\Phi_{\tau+s,rg}$
1	0.0442	0.0373	94	47	209
1	0.0214	0.0533	200	100	444
1	0.0431	0.0545	366	184	813
1	0.0657	0.0539	823	413	1829
1	0.0439	0.0750	869	436	1931
2	0.0629	0.0321	98	79	145
2	0.0316	0.0474	205	166	304
2	0.0630	0.0474	389	315	576
2	0.0630	0.0653	851	688	1260
3	0.0390	0.0302	111	22	748
3	0.0204	0.0439	223	44	1509
3	0.0394	0.0437	417	82	2824
3	0.0589	0.0439	856	168	5787
3	0.0391	0.0593	922	181	6240
4	0.0462	0.0322	99	42	305
4	0.0230	0.0475	213	90	655
4	0.0456	0.0474	390	165	1200
4	0.0679	0.0468	868	367	2671
4	0.0461	0.0650	889	376	2736

Table 2: Operating conditions for the various inserts were chosen so as to keep the momentum flux ratio $\Phi_{\tau,rg}$ constant across geometries.

height; the size of this change varies with operating condition and geometry. Consequently, strong estimates of the uncertainty in the length measurements are very difficult. Here length error bars here are set to a fixed value (+/-1.20 mm) based on the effect of the noncrisp border and repeatability studies.

Results and Discussion

Test conditions are given in Table 2. The conditions were chosen to represent a range of mass flows while maintaining the gas-to-liquid momentum flux ratio across geometries. The momentum flux ratio ($\Phi_{\tau,rg}$) was defined using the dimensions just prior to the end of the sheltering lip—$\left(m_g/m_\ell\right)^2\left(\rho_\ell/\rho_g\right)\left[\tau\left(2r_o-\tau\right)/r_g^2\right]^2$ where m represents the mass flow rate and ρ is the density. As noted in the introduction, the momentum flux ratio was chosen because it is believed to be the main factor for determining atomization rate based on investigations of other atomizer types [5-7] and a model of stripping atomization developed for GCSC injectors [4]. A series of five $\Phi_{\tau,rg}$ were investigated for each of the four injector inserts. At all of these operating conditions a solid-cone spray was formed. At the lower momentum flux ratios a hollow cone of very large droplets (likely 0.25 mm or larger) was formed on the outer periphery of the spray. This cone of larger droplets had a much greater spray angle than the inner, solid cone; by eye this spray angle appears close to the angle of the hollow cone produced by operating the injector with no gas flow. No measurement of droplet sizes has yet been made, but the droplets in the solid cone are of a size typically seen in rocket injectors, probably with an SMD on the order of 10's of microns. As expected, higher momentum flux ratios appeared to produce smaller droplets.

The energy of the gas flow is the driving force for atomization in these injectors. As such, the film length (L) should decrease as the gas becomes more energetic (compared to the liquid). In other words, the L should decrease as Φ increases. This trend is observed in all of the geometries tested (see Fig. 4). The momentum flux may be defined in several ways depending on the characteristic dimension chosen to calculate fluid velocities from mass flow rates. The gap height, τ, strongly controls the velocity vector of the liquid and, therefore, effects the relative velocity between the gas and the liquid (although the gas velocity still dominates this ratio). The bulk velocity of the gas is mainly controlled by r_g. However, given that the bulk flow expands prior to actual contact with the liquid and to account, in part, for the lower velocity in the recirculating gas, r_g+s (which is

identically r_o-τ) seems a more likely choice. Figure 4 shows the nondimensional film length (L/τ) as a function of this momentum flux ratio, $\Phi_{\tau,rg+s} = (m_g/m_\ell)^2 (\rho_\ell/\rho_g)[\tau(2r_o-\tau)/(r_o-\tau)^2]^2$. The data appear to collapse onto a single curve using these parameters. This characteristic gas dimension differs from the one originally chosen when designing the experiments. Initially, the effect of the expansion on gas velocity was expected to minimally impact atomization, but the results show that the effect is appreciable. It is interesting to note, however, that plotting L/τ as a function of the original momentum flux ratio, $\Phi_{\tau,rg} = (m_g/m_\ell)^2 (\rho_\ell/\rho_g)[\tau(2r_o-\tau)/r_g^2]^2$, produces a series of curves with the same behavior (e.g., slope) but differing absolute values (Fig. 5).

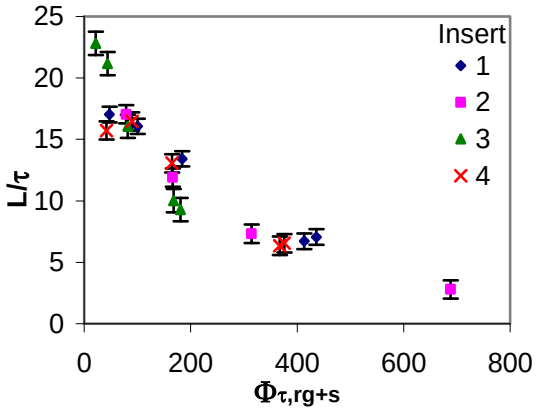

Figure 4: The nondimensional film length is shown as a function of $\Phi_{\tau,rg+s}$.

Studies of other gas-phase dominated injectors suggest that film length should vary as a function of air-to-liquid ratio (m_g/m_l) or gas or liquid velocity [8-10]. The current experiments do not show any correspondence between air-to-liquid mass flow ratio, ratio of Reynolds numbers, the gas or liquid Reynolds number (singly) or the individual velocities in these GSCS injectors. Numerous possible characteristic dimensions were investigated for defining these parameters and nondimensionalizing the film length, e.g. τ, τ+s and measured maximum film height, h. The main driving force affecting atomization rate and, therefore, film length does indeed appear to be the momentum flux ratio.

Figure 4 also shows that the trend for L/τ versus $\Phi_{\tau,rg+s}$ is not linear. The length seems to asymptote to a minimum value. This behavior is likely due to the interaction of the separation bubble and the liquid film; a simplified diagram of this interaction is shown as Fig. 6. It appears that when the liquid is in contact with the bulk gas flow, its length is very sensitive to the momentum flux ratio. The length of the film in contact with the recirculation zone seems to be largely dominated by the reattachment length. As the film shortens, a smaller percentage of the liquid is in contact with the bulk gas flow, i.e. the region labeled "Φ-dominated zone" in Fig. 6. The smaller the percentage of film in contact with the Φ-dominated zone, the less sensitive the film length is to changes in the momentum flux ratio—the length is largely controlled by the reattachment length. The exact cause for this two-regime set-up is currently unknown and study is complicated by the unknown behavior of a separation bubble in contact with a wall-bounded liquid. Investigations of recirculation-zone effects on atomization have been mainly limited to jets and sheets and have not studied the changes in reattachment behavior due to the existence of the liquid. In these studies recirculating flows can have a steadying effect on the flow decreasing atomization [11], or they can enhance atomization by driving instabilities [12].

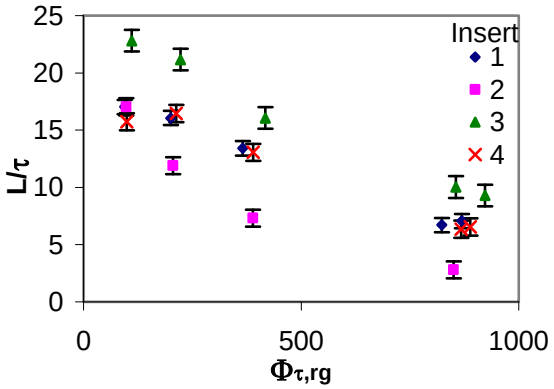

Figure 5: The nondimensional film length is shown as a function of the $\Phi_{\tau,rg}$. The inserts show the same general trends, but differing absolute values

The complexity of a separation bubble in contact with a wall-bounded liquid can be seen from earlier CFD simulations of similar injectors [1]. In these simulations the sheltering lip creates a separated flow which, as a result of lower pressure and possibly a result of drag forces from the recirculating flow, causes the liquid to partially fill the separation bubble (see Fig. 6 & 7). In other words, the liquid thickness just downstream of the sheltered area (h) is greater than the height under the sheltering lip, τ.

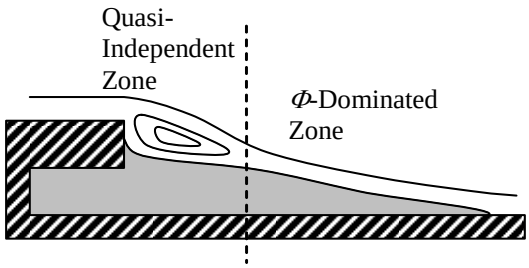

Figure 6: A notional diagram shows the outlet section of the injector (hashed), the film (gray) and the streamlines of the separated gas. The quasi-independent zone is the area of the film in contact with the recirculation zone; the Φ-dominated zone is in contact with the bulk flow.

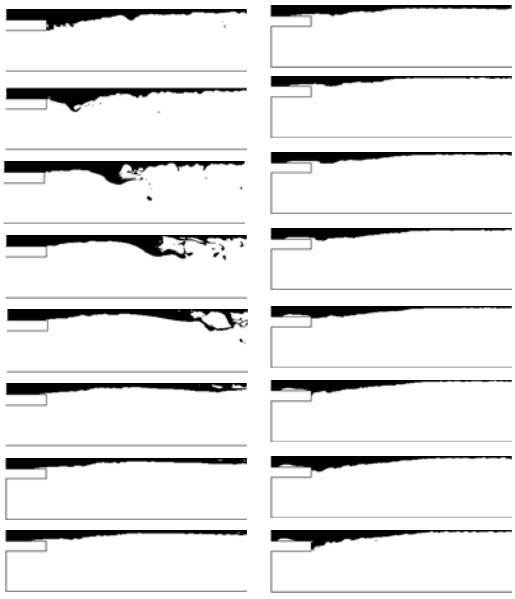

Figure 7. Axisymmetric simulation of insert 4 with $\Phi_{\tau,rg+s}$=42. Flow is from left to right. The black region represents the liquid; only half of the injector is shown. Images are given at 1.5×10^{-3} s intervals from top to bottom then left to right. More details regarding these simulations may be found in [1].

This initial increase in film thickness is seen in the experiments. The CFD results show that this recirculation zone is unstable under many conditions [1, 2]. In the two-phase simulations the interaction of the liquid and gas near the sheltering lip cause the recirculation zone to be shed producing a wave of fluid (see Fig. 7). No large wave-like structures were observed in these experiments, although earlier

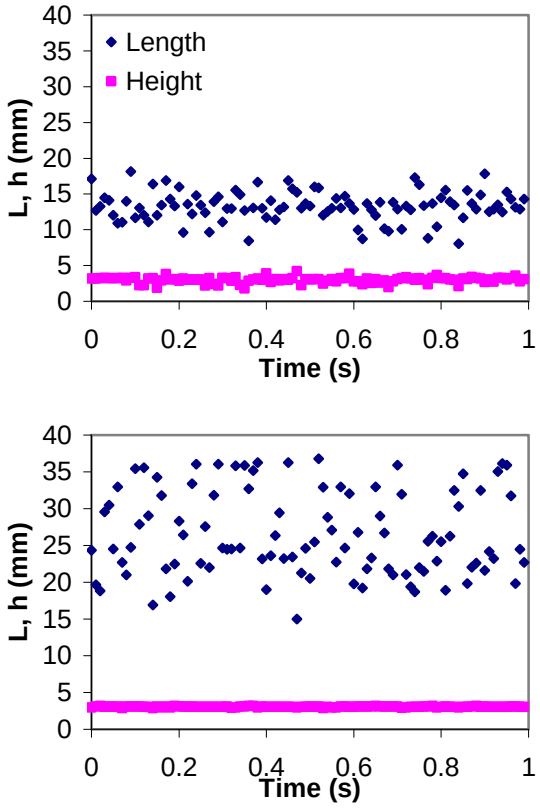

Figure 8: Temporal variation of L and t is shown for two $\Phi_{\tau,rg+s}$—413 (a) and 184 (b).

experiments with a sharply tapered lip did show evidence of occasional liquid pulses where the film thickened [1]. The current set of experiments shows a different type of pulsing in which a long tongue of fluid is occasionally produced (see Fig. 3). Variations in the initial film height were also evident. Changes in the film height will clearly alter the recirculation zone and should have an effect on film length. While no sudden downstream increase in film thickness were observed, the experimental results do show slight increases and decreases in *h* with occasional, sudden decreases in film height which mimic some of the CFD findings (Fig. 7) (although *h* never decreases to the extent seen in the simulations). Again, this suggests that the film escapes under the recirculation zone instead of over it and helps explain the tonguing behavior. If the recirculation and change in h is truly responsible for the appearance of short-lived tongues of film then there should be some correlation between *L* and *h* in time. A plot of *L* and *h* versus time is given as Fig. 8. No correspondence of a sudden decrease in *h* with a sudden increase in *L* was seen in these data; not

even a phase-shifted correspondence could be found. However, the data rate was limited to 100 images/second which may be too slow to capture the behavior. Future, higher speed, experiments are planned which should help discover the relationship between the two. Also of note, the unsteadiness in h and L is observed at all momentum ratios, but the flow appears to be more stable at higher momentum flux ratios (see Figs 8a and 8b, for example). The tonguing behavior is mainly observed at high Φ; at low Φ a different anomaly in film profile is occasionally observed—a sharp decrease in film thickness at the trailing edge of the film. At low Φ some frames contain films whose thickness varies from near τ to 0 over a distance of 1.25 mm or less. This behavior may be another type of pulsing where a "wall" of liquid is suddenly sent downstream or may result from the loss of a large chunk of liquid due to the downstream shedding of the recirculation zone. The apparent relationship between height and length suggest that the recirculation zone may create a barrier to the liquid flow. This barrier would be expected to have more pronounced effect at higher Φ where the gas-phase energy dominates the liquid-phase energy. The asymptotic behavior of L/τ and the existence of the two zones depicted in Fig. 6 are likely the result of this barrier effect.

Despite the frame-to-frame variations in h, there appears to be little or no correlation between measured h and L on the average; this is evidence by the scaling of L with τ only (not h or τ+s). To help understand some of the impact of the separated flow, attempts are made to correlate h with the geometry and operating conditions of the injector. The maximum film height, h, can reasonably be expected to relate to s. However, a plot of measured h versus s does not appear to show any correspondence. This lack of correspondence likely results from the fact that the film decreases in height as it moves downstream, eventually decreasing to nothing (see Fig. 11). The gas flow reattaches at some point downstream when the film is an unknown height, possibly zero (see Fig. 6). Since a straightforward nondimensionalization is desired, the film is considered to be gone, i.e of zero height, by the time the gas reattaches: in this situation, the relevant height is more plausibly τ+s. The initial film height does indeed show some correspondence with τ+s (Fig. 9). This suggests that atomization while the liquid is in the quasi-independent zone is not entirely negligible even though it is slower than when the liquid is in the fast zone. The initial film height does not depend on momentum flux ratio (Fig. 10) despite the variation of film thickness with momentum flux (Fig. 11); consequently, the unknown height of the liquid at the reattachment point does not appear to be a concern. The scatter in the points at a given τ+s is likely the result of Reynolds number and boundary layer effects on the reattachment [13]. The differing geometry of the gas inlet across the different inserts creates unavoidable boundary layer changes.

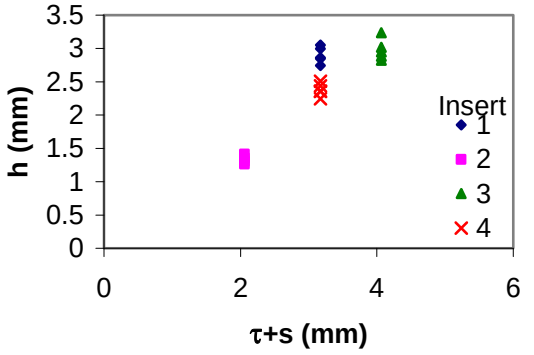

Figure 9: Measured film height just downstream of the sheltering lip (0.94 mm) is shown versus the step height plus the gap height. The data show the expected rising trend for measured height versus step plus gap height.

Conclusions

The results of a parametric study of film length in gas-centered swirl-coaxial injectors were presented. It was observed that the liquid film length decreases as the momentum ratio increases—the more energetic gas being more affecting at removing liquid from the interface. Because the atomization rate is dominated by the energies (equivalently the

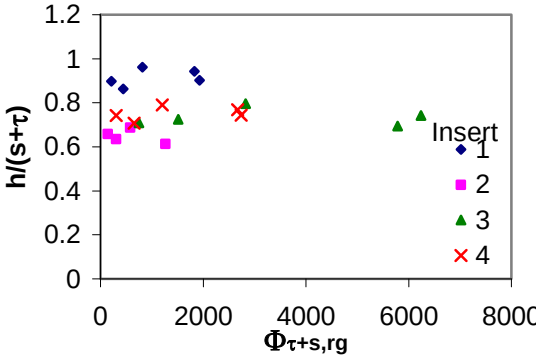

Figure 10: Nondimensional h is independent of the momentum flux ratio. Here $\Phi_{\tau+s,rg}\left(m_g/m_\ell\right)^2\left(\rho_\ell/\rho_g\right)\left[(\tau+s)(2r_o-\tau-s)/r_g^2\right]^2$, which is reflective of the choice of step plus gap height as the characteristic liquid dimension. Other definitions of momentum flux show the same results.

Figure 11: The profile of the film with insert 1 at $\Phi_{\tau,rg}$=413 (black) and $\Phi_{\tau,rg}$=184 (grey).

momentum fluxes) in the system, the film length scales with the characteristic dimension used to determine the bulk velocities of the phases—τ for the liquid and r_g+s for the gas. The film length does not decrease linearly with $\Phi_{\tau,rg+s}$ but appears to approach an asymptote. This behavior is likely due to the increasing percentage of film in contact with the recirculating flow as the momentum flux ratio increases. The bulk flow seems to have a much greater impact on film length than the recirulating flow. This behavior appears to be the main impact of the recirculation on the film length in an average sense and is thought to result from the reattachment of the gas creating a sort of barrier to liquid flow.

Evidence of a barrier effect is seen in transient film thickness behaviors such as tonguing. However, no correlation between changes in h and L, with respect to time, was evident in these data. While this finding likely results from the low frame rate of the data, it may indicate that the two measurements are not coupled. Further investigations will be conducted at higher frame rates. On average, h is related to τ+s and does not appear to impact the average length of the film. Finally, the height scaling is not affected by the momentum ratio over the range tested here, although there is some scatter in the data thought to relate, in part, to changes in boundary layer thickness.

Acknowledgements

The assistance of Matt Billingsley (AFRL), Dave Hill (ERC) and Earl Thomas (ERC) in conducting these experiments is appreciatively recognized.

References

[1] Lightfoot, M. D. A., Danczyk, S. A. and Talley, D. G., *19th ILASS Americas Annual Conference on Liquid Atomization and Spray Systems*, Toronto, ON Canada, May 2006.

[2] Canino, J., Heister, S., Sankaran, V. and Zakharov, S., AIAA-2005-4297, *41st AIAA/ASME/SAE/ASEE Joint Propulsion Conference and Exhibit*, Tucson, AZ, July 10-13 2005

[3] Strakey, P., Cohn, R. K. and Talley, D. G., *17th ILASS Americas, Annual Conference on Liquid Atomization and Spray Systems*, Arlington, VA, May 16-19 2004.

[4] Lightfoot, M. D. A., Danczyk, S. A. and Talley, D. G., *20th ILASS Americas Annual Conference on Liquid Atomization and Spray Systems*, Chicago, IL, May 2007.

[5] Carvalho, I. S., Heitor, M. V. and Santos, D., *International Journal of Multiphase Flow* 28:773-789 (2002).

[6] Lozano, A. and Barreras, F., *Experiments in Fluids* 31:367-376 (2001).

[7] Mayer, W. O. H., *Experiments in Fluids* 16:401-410 (1994).

[8] Chin, J. S., Rizk, N. K. and Razdan, M. K., *Journal of Propulsion and Power* 16:297-301 (2000).

[9] Lavergne, G., Trichet, P., Hebrard, P. and Biscos, Y., *Journal of Engineering for Gas Turbines and Power-Transactions of the ASME* 115:461-466 (1993).

[10] Schmidt, U. T. and Sojka, P. E., *Atomization and Sprays* 9:173-192 (1999).

[11] Park, J., Huh, K. Y., Li, X. and Renksizbulut, M., *Physics of Fluids* 16:625-632 (2004).

[12] Lopez-Pages, E., Dopazo, C. and Fueyo, N., *Journal of Fluid Mechanics* 515:1-31 (2004).

[13] Adams, E. W. and Johnston, J. P., *Experiments in Fluids* 6:493-499 (1988).